Ophthalmology Clinics & Research
OCR, 3(1): 131-138
www.scitcentral.com

ISSN: 2638-115X

Original Research Article: Open Access

Magnetic Resonance Imaging and Ultrasound in the Follow Up of Patients Treated for Choroidal Melanomas: Do They Correlate?

Al-Wassia R[1,2*], Goncalves FG[1,3], Holly C[4], Chankowsky J[5], Ahamed NAB[2] and Shenouda G[1*]

*[*1]Department of Radiation Oncology, McGill University Health Center, Montréal, Québec, Canada*

*[*2]Department of Diagnostic Radiology, King Abdul-Aziz University, Jeddah, Saudi Arabia*

[3]Department of Diagnostic Radiology, Brasília Children Hospital, Brasília, Brazil

[4]Division of Infectious Disease and Department of Psychology, The Ottawa Hospital, Ottawa, Ontario, Canada

[5]Department of Diagnostic Radiology, McGill University Health Centre, Montréal, Québec, Canada.

Received December 10, 2019; Accepted January 03, 2019; Published April 09, 2020

ABSTRACT

Objective: Selection of treatment for choroidal melanoma relies upon an accurate determination of the size, and location of the lesion. Currently, fundoscopic ultrasound (US) is the gold-standard measurement modality; however, magnetic resonance imaging (MRI) may be a useful alternative tool in the assessment and follow-up of choroidal melanoma. The goal of the current study was to correlate the MRI and US measurements performed for patients diagnosed with peripapillary choroidal melanoma who underwent both modalities in their follow up after fractionated stereotactic radio surgery (SFRT).

Design: Retrospective chart review.

Subjects: Forty-three patients diagnosed with choroidal melanoma that were treated with SFRT.

Methods: The charts of patients, diagnosed with peripapillary choroidal melanoma and treated with SFRT at McGill University Center between April 2003 and December 2009, were reviewed. Each patient had an US and MRI of the orbit before treatment. The authors used high resolution MRI to retrospectively measure the height (anterior-posterior) and base diameters of each lesion. The MRI measurements were performed by an expert neuro-radiologist, while the ultrasound scans were interpreted by an expert ophthalmologist specialized in the field. Both of the neuro-radiologist and the ophthalmologist were blinded to the results of the other modality. Ultrasound and MRI measurements were statistically compared using the Bland and Altman approach.

Main outcome measures: Tumor measurements on ultrasounds and MRIs scan.

Results: A strong agreement between both techniques was observed. Correlations for the measurements ranged from 0.85 (sagittal gadolinium) to 0.88 (axial T1, axial T2, sagittal T2). Tumor size determined by ultrasound was larger than that measured by MRI (sagittal MRI; axial T2; $p<0.01$). Overall, there was good agreement between ultrasound and axial T1 anterior-posterior, sagittal and axial post gadolinium measurements.

Conclusion: Magnetic resonance imaging measurements correlated well with those measured on ultrasound scans. Our findings suggest that MRI may be a useful imaging modality to assess response to treatment and to follow-up patients with peripapillary choroidal melanomas treated with SFRT.

Keywords: Magnetic resonance imaging, Ultrasound, Choroidal melanomas, Stereotactic radio surgery

Corresponding author: Rolina Al-Wassia, Department of Diagnostic Radiology, King Abdul-Aziz University, Jeddah, Saudi Arabia, E-mail: ralwassia@kau.edu.sa

George Shenouda, MD, PhD, Department of Radiation Oncology, McGill University Health Cente, 1650 Cedar Avenue, Montreal, Québec, Canada, H3G 1A4, Tel: 514 934 8040, Fax: 514 934 8592, E-mail: george.shenouda@muhc.mcgill.ca

Citation: Al-Wassia R, Goncalves FG, Holly C, Chankowsky J, Ahamed NAB, et al. (2020) Magnetic Resonance Imaging and Ultrasound in the Follow Up of Patients Treated for Choroidal Melanomas: Do They Correlate? Ophthalmol Clin Res, 3(1): 131-138.

INTRODUCTION

Choroidal melanoma (CM accounts for 85 to 90% of all uveal melanomas, with an annual incidence of 6 to 8 cases per million people) [1]. Choroidal melanoma is the commonest primary intra-ocular malignancy in adults [1] with a predilection for Caucasians [2]. An increase in incidence is noted with age, and less than 2% cases are noted <20 years old [3].

The Collaborative Ocular Melanoma Study (COMS) categorizes CM into small, medium or large based on the largest basal diameter (LBD) and height of the tumor [4]. Small CMs range from 1.0 mm to 3.0 mm in apical height and have an LBD of 5.0 to 16.0 mm [5]. Medium CMs range from 3.1 to 8.0 mm in apical height and have a basal diameter of ≤ 16.0 mm. Large CMs are >8.0 mm in apical height or have a basal diameter >16.0 mm when the apical height is at least 2.0 mm.

Initial diagnosis of CM is made after careful ophthalmological examination combined with noninvasive ancillary tests such as ocular ultrasound. Ultrasound is considered the gold standard method for diagnosis and measurements [6,7].

The management of CM is aimed at controlling the tumor (with organ preservation), preventing metastasis and, ultimately, increasing overall survival. The choice of the treatment modality depends on tumor size and location (distance from the optic nerve) and various alternatives exist, including photocoagulation, trans pupillary thermotherapy [8], photodynamic therapy [9], endoresection, enucleation, and radiotherapy [10,11].

Previously, the standard treatment for CM was enucleation for CMs of all sizes [11]. Subsequently, randomized controlled clinical trials demonstrated no advantage of enucleation over eye-conserving plaque brachytherapy in reducing metastasis and improving survival in patients with medium-size CMs [12]. Currently, the management of small- and medium-size CMs aims at controlling the tumor with organ preservation. Furthermore, the COMS reported that pre-enucleation irradiation did not improve survival in patients with large CMs [13].

Radiotherapy in the form of radioactive plaque brachytherapy or external beam radiotherapy is the standard eye-conserving treatment for medium-size CMs [11,14,15]. The general consensus is that peripapillary lesions located within 2 mm from the optic nerve head should not be treated by radioactive plaque brachytherapy, as high-dose in close proximity to the surface of the plaque applicator would cause significant damage to the optic nerve. Proton therapy, gamma knife or stereotactic radiotherapy are commonly used treatment options for tumors located ≤ 2 mm from the optic disk [15,16].

At McGill University Health Center, patients with peripapillary choroidal melanoma are offered fractionated stereotactic radiotherapy as a treatment option. Stereotactic radiotherapy planning is performed with magnetic resonance imaging (MRI) scan of the orbit with Gadolinium. MR and CT scans are used for planning and co-registration using thin slice thickness <2 mm for both. The gross tumor volume (GTV) consisted of a composite volume, including the lesion in axial, coronal and sagittal projections, using both T1- and T2-weighted MRI sequences.

In our experience, when the planning CT scan was co-registered with the orbit MRI, GTV contouring was significantly improved, as the tumor was well defined and the contours of organs at risk (optic nerve, lacrimal gland, and lens) were well delineated. A planning target volume (PTV) was obtained by a 3-D expansion of 3 mm around the GTV.

Follow-up included history and physical examination, visual acuity, ocular ultrasound, slit-lamp examination, tonometry, fundoscopy and fluorescence angiography at 3 months intervals. A tour centre, we included MRI of the treated orbit as an additional modality to assess response to radiotherapy.

In this report, we compared measurements obtained by ocular ultrasound with those obtained by MRI in order to determine whether both measurements were correlated.

PATIENTS AND METHODS

Patients with peripapillary CM who were treated with stereotactic radiotherapy were identified from the hospital records of Montreal General Hospital (McGill University Health Centre) and Notre Dame Hospital (Centre Hospitalier de l'Université de Montréal). Data were obtained from 43 patients (26 females, 17 males) who were treated between July 22, 2003 and November 10, 2010.

Overall 115 pairs of ultrasound and MRI data were obtained from participants having measurements for tumor height (AP) taken in the previous 12 months, with an average time interval between ultrasound and MRI exam of 92 days. The median age of patients was 69 years (range 30-92 years). Eighty four percent of the patients had medium-size lesions (apical height, 3-10 mm and basal diameter, 5-16 mm) and 16% had small lesions (apical height, <3 mm and basal diameter, 5-16 mm) based on the Collaborative Ocular Melanoma Study (COMS) classification [16]. All lesions were located within 2 mm from the optic disc. Prior to treatment, staging procedures, including physical examination, blood tests, chest X-ray and abdominal ultrasound were performed in all patients to exclude distant metastasis.

Two independent physicians, an ophthalmologist and a neuro-radiologist, assessed patients' response to therapy using three dimensional ocular US and MRI with gadolinium. The ophthalmologist interpreted ocular

ultrasound findings, while the neuro-radiologist interpreted MRI examinations. Both the ophthalmologist and the neuro-radiologist were blinded to the results of assessment obtained by the other modality. This research was approved by the Institutional Review Board of Montreal General Hospital and by the Comité d'évaluation scientifique of Notre Dame Hospital.

STATISTICAL Analysis

Statistical analysis was performed using the Statistical Package for the Social Sciences (SPSS, Chicago, IL, USA), version 17.0. To detect statistically significant differences between continuous variables (MRI and US), paired t-tests were applied. The Bland and Altman approach [17] was used to compare ultrasound and MRI measurements of tumor height by calculating the mean and standard deviation (SD) of the difference. Bland and Altman's approach was designed to enable medical researchers to compare two methods of measurement - in this case, to compare a proposed new method of measurement with a previously existing one. This statistical analysis determines whether these two methods can be used interchangeably or whether the new method can replace the old one. In summary, this method visually provides the difference scores of two measurements against the mean and allows the evaluation of agreement between the two measurement tools [18]. This method has been widely reported and its utility has been demonstrated in both clinical and laboratory studies [17].

From our data, the mean difference between ultrasound and MRI was calculated along with the limits of agreement (mean ± 2SD). Two-tailed significance was set at 5%. Ninety-five percent confidence intervals (95% CI) were calculated as ± 2SD. Bland-Altman plots were created to show the level of agreement between the measurement tools.

RESULTS

Ultrasound and MRI measurements of the patients are provided in **Table 1**.

Table 1. Axial T2 AP measurement is the most accurate within this set of MRI measurements.

	Mean difference	T value	Correlation
US H × Sag T2 AP	0.39 ± 0.88	4.82	0.880
US H × Sag T1 AP	0.34± 0.93	3.95	0.873
US H × Axial T1 AP	0.08± 1.1	0.895	0.879
US H × Axial T2 AP	0.30± 0.99	3.22	0.884
US H × Sag Gado	-0.11 ± 1.2	-0.909	0.846
US H × Axial Gado	0.11±097	1.17	0.867

Abbreviations: AP: Anteroposterior; Gado: Gadolinium; H: Height; Sag: Sagittal; US: Ultrasound
**Data are presented as mean and standard deviation unless otherwise specified*

Tumor size measurements obtained by ultrasound were larger than those obtained on sagittal (both T1 and T2), $p<0.01$ and axial MRI scans T2 AP measurement, $p<0.01$. Overall, significant differences were not found between ultrasound and axial T1 anterior-posterior, sagittal and axial gadolinium measurements **(Table 2)**; however, we did find a strong agreement between the 2 modalities for these measurements. These findings are confirmed by the limits of agreement provided in the Bland-Altman plots **(Figures 1-6)**. **Figures 7 and 8** demonstrate the MRI in axial (A) and sagittal (B) T2-weighted images showing anterior-posterior (height of the tumor) with and without gadolinium.

Table 2[1]**.** Paired sample t-tests between US and MRI measurements.

	Mean		US-MRI (%)[2]	P value
US height	4.04	1.77		
Sag T2 AP	3.65	1.84	10.7%	<0.001
Sag T1 AP	3.75	1.88	8.3%	<0.001
Axial T1 AP	3.98	2.21	1.5%	0.373
Axial T2 AP	3.7	32.1	8.3%	0.002
Sag Gado	3.98	1.94	-3.6%	0.365
Axial Gado	4.18	2.31	1.5%	0.242

Abbreviations: AP: Anteroposterior; Gad: Gadolinium; H: Height; MRI: Magnetic Resonance Imaging; Sag: Sagittal; U: Ultrasound
[1]Data are presented as mean unless specified otherwise
[2]Positive values indicate higher ultrasound values

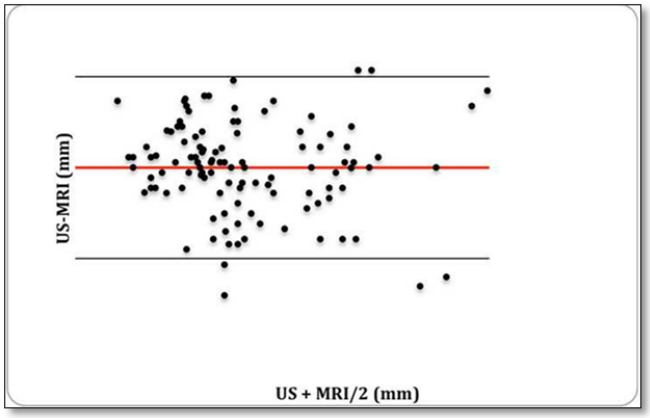

Figure 1. A Bland-Altman plot of mean values for tumor size (mm) determined by ultrasound (US) versus magnetic resonance imaging (MRI; sagittal T2-weighted) for all subjects (n=115). Mean of difference was 0.40 mm; standard deviation (SD) of difference was 0.89 mm and limits of agreements were mean -1.96 × SD=-1.38 mm and mean +1.96 × SD=2.17 mm.

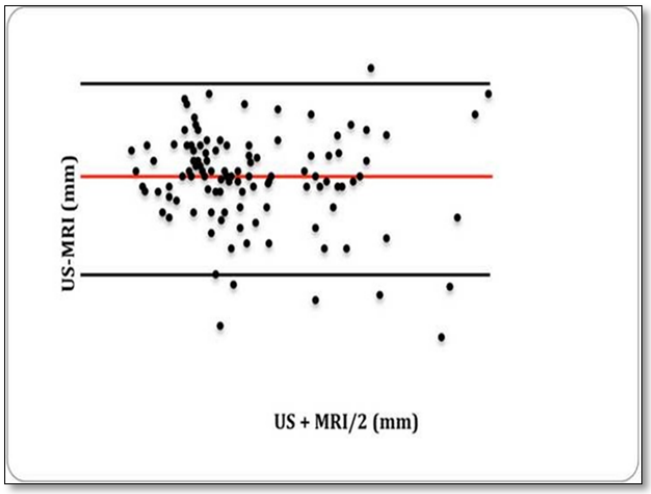

Figure 2. A Bland-Altman plot of mean values for tumor size (mm) determined by ultrasound (US) versus magnetic resonance imaging (MRI; sagittal T1-weighted) for all subjects (n=113). Mean of difference was 0.34 mm; standard deviation (SD) of difference was 0.93 mm and limits of agreements were mean -1.96 × SD=-1.51 mm and mean +1.96 × SD=2.20 mm.

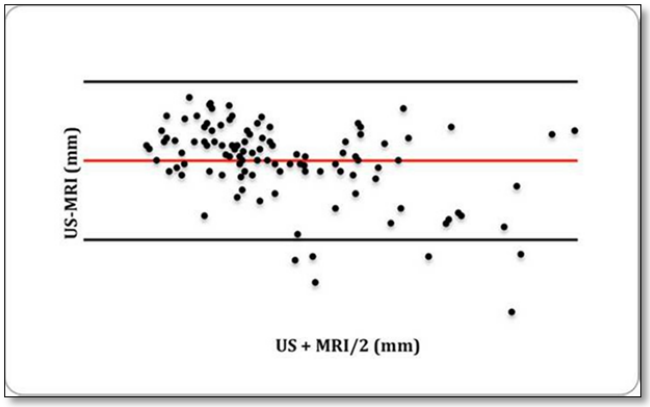

Figure 3. A Bland-Altman plot of mean values for tumor size (mm) determined by ultrasound (US) versus magnetic resonance imaging (MRI; axial T1-weighted) for all subjects (n=114). Mean of difference was 0.09 mm; standard deviation (SD) of difference was 1.07 mm and limits of agreements were mean -1.96 × SD=-2.05 mm and mean +1.96 × SD=2.22 mm.

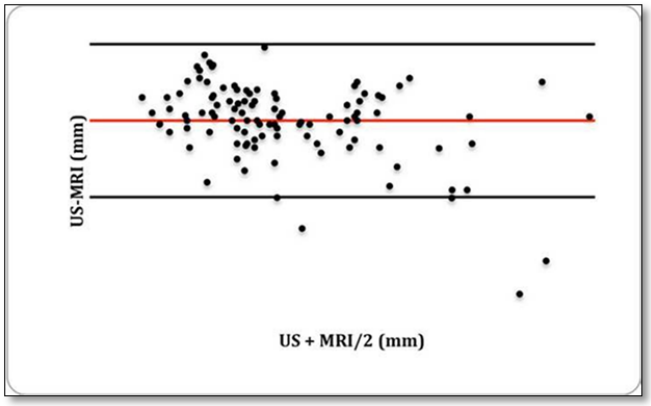

Figure 4. A Bland-Altman plot of mean values of tumor size (mm) determined by ultrasound (US) versus magnetic resonance imaging (MRI; axial T2-weighted) for all subjects (n=113). Mean of difference was 0.30 mm; standard deviation (SD) of difference was 0.99 mm and limits of agreements were mean -1.96 × SD=-1.69 mm and mean +1.96 × SD=2.28 mm.

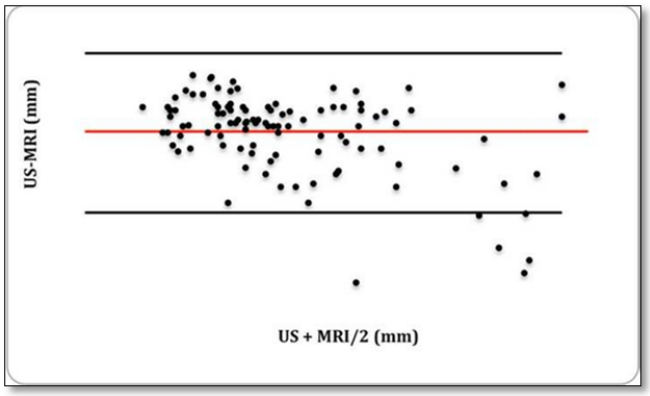

Figure 5. A Bland-Altman plot of mean values of tumor size (mm) determined by ultrasound (US) versus magnetic resonance imaging (MRI; axial gadolinium- enhanced) for all subjects (n=112). Mean of difference was -0.11 mm; standard deviation (SD) of difference was 1.25 mm and limits of agreements were mean -1.96 × SD=-2.61 mm and mean +1.96 × SD=2.39 mm.

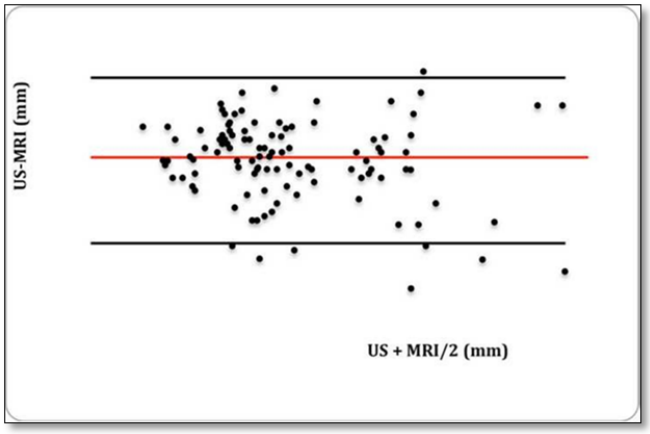

Figure 6. A Bland-Altman plot of mean values of tumor size (mm) determined by ultrasound (US) versus magnetic resonance imaging (MRI; sagittal gadolinium- enhanced) for all subjects (n=112). Mean of difference was 0.11 mm; standard deviation (SD) of difference was 0.97 mm, and limits of agreements were mean −1.96×SD=−1.84 mm and mean +1.96 × SD=2.05 mm.

Figure 7. Magnetic resonance images (A) axial and (B) sagittal T2 weighted image showing anterioposterior (height of the tumor).

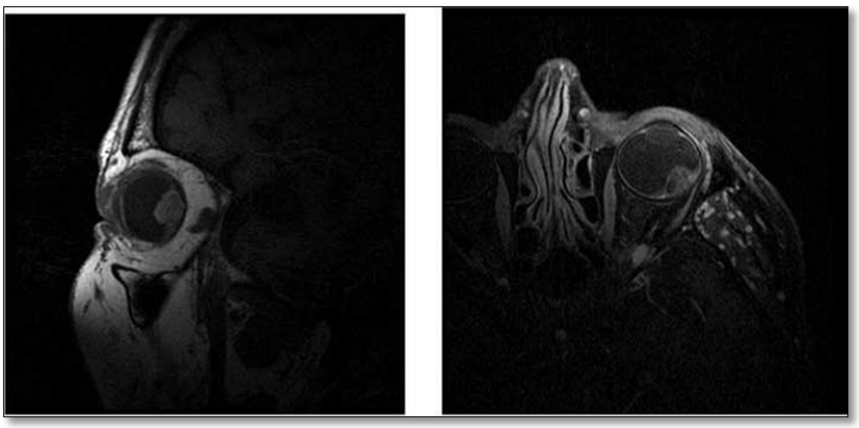

Figure 8. Magnetic resonance images (A) axial and (B) sagittal T1 weighted image with gadolinium showing anterioposterior (height of the tumor).

DISCUSSION AND CONCLUSION

Historically, CMs have been evaluated by fundoscopy and fluorescein angiography. However, ultrasonography has emerged as a gold standard for detecting and following up CM. A combination of both A-mode and B-mode ultrasonography is important. On A-scan ultrasonography, CMs show medium to low internal echoes, with or without intratum oral vascular pulsations. On B-scan, three distinct features are demonstrated: (1) an acoustic anechoic zone within a lesion of intermediate echogenicity, (2) choroidal excavation, and (3) shadowing in the orbit. When lesions are <3 cm, then images A and B mode sonography in combination is shown to give greater results [19]. There were no systematic errors in patients with tumor size <6 mm, rather a trend of MRI to underestimate ultrasound measurements without an indication of a systematic error. Above 6 mm, the measurements appeared to be less accurate; however, this error also does not appear to be systematic and rather could be indicative of measurement error. In these instances it appears that it is a larger tumor positioned on an uncommon axis, which resulted in the true tumor size not being captured between two planes of MRI measurements and significantly underestimated though this is a rare occurrence. This only becomes an issue with larger tumors when the peak of the tumor is lost between two planes or due to volume averaging, hence showing large differences between the US and MRI measurements. Overall, findings indicate that MRI is a reliable substitute for US measurements and that the axial T2 AP measurement is the most accurate within this set of MRI measurements. Future studies however will be prospective allowing for further investigation if significant differences occur between these measurements and it is recommended that the plane slices occur at 1mm intervals to minimize the risk of the peak height occurring between two planes. The advent of MR magnet advancement has given many high resolution 3D isotropic sequences which may be utilized in better segmentation and contouring of the lesions.

Magnetic resonance imaging of the orbits is an excellent modality in assessing orbital pathology. The standard practice of three orthogonal plane 3 mm fat-saturated T2-weighted images, axial and coronal T1-weighted images with fat saturations are useful in assessing melanomas.

Additional orthogonal imaging with contrast adds value in distinguishing the lesions from the uveal margins.

The MR characteristic features of melanomas are due to the paramagnetic effects of melanin, which result in shortening of T1 and T2 relaxation times [20]. This shortening effect is attributed to a combination of effects by the unpaired electrons in the free radicals and the chelated metal ions present in melanin due to dipole-dipole interactions.

The T2 hypo-intensity is probably due to the lesion's high cellularity and to the tightly cohesive bundles between cells. Other histologic features may also contribute to some degree of T2 signal heterogeneity such as hemorrhage and necrosis [21].

Given these MR considerations, CMs show hyper-intensity in relation to the cortex on T1-weighted images, hypo-intensity relative to the cortex on T2-weighted images, hyper-intensity or iso-intensity relative to the cortex on proton density-weighted imaging. These are often associated with sub-retinal hemorrhage, which is best assessed on T2-weighted images, where-in they appear as a hyper intese rim of fluid. Fat saturation techniques and paramagnetic contrast are useful to assess extra-ocular extension (Tenon's capsule and into the optic disc) and to distinguish the lesion itself from retinal detachment or hemorrhagic sub-retinal fluids [20-22].

Given the retrospective nature of our study, we were unable to obtain measurements as closely timed together as possible. Of note, these tumors are extremely slow growing and a significant change in dimension over short intervals of time may be radiologically assessed by neither ultrasonography nor MRI.

Our onus of choosing MR is that with the advent of an exponential increase in MR technology, as well as in hospital budgeting, MR is more widely available, and, more importantly, reliably reproducible. Although relatively cheaper, ultrasound examinations should be performed by skilled personnel. Further, the reproducibility of ultrasound examinations is questionable, particularly in cases of follow-up examination.

For better assessment, we recommend, in addition to the standard sequences for orbital assessment of the orbits, three-dimensional constructive interference in steady state (CISS) sequence and analysis with any commercially available reconstruction workstation software for MR protocols. Being a T2 gradient sequence, CISS gives good T2 differentiation of tumor versus the rest of the uveoscleral structures. Moreover, segmentation could be applied to calculate tumor volume. We believe this would be a better assessment of interval growth than two-plane measurement of the lesion, which is prone to error as the image acquisition planes on follow-up scans cannot be matched.

REFERENCES

1. Egan KM, Seddon JM, Glynn RJ, Gragoudas ES, Albert DM (1988) Epidemiologic aspects of uveal melanoma. Surv Ophthalmol 32:239-251.
2. Isiklar I, Leeds NE, Fuller GN, Kumar AJ (1995) Intracranial metastatic melanoma: Correlation between MR imaging characteristics and melanin content. AJR Am J Roentgenol 165: 1503-1512.
3. Byrne SF, Green RL (2002) Ultrasound of the eye and orbit. Mosby Year Book.
4. Collaborative Ocular Melanoma Study Group (2003) Trends in size and treatment of recently diagnosed choroidal melanoma, 1987-1997: Findings from patients examined at collaborative ocular melanoma study (COMS) centers: COMS report no. 20. Arch Ophthalmol 121: 1156-1162.
5. Collaborative Ocular Melanoma Study Group (1997) Factors predictive of growth and treatment of small choroidal melanoma: COMS report no. 5. Arch Ophthalmol 115: 1537-1544.
6. Collaborative Ocular Melanoma Study Group (1990) Accuracy of diagnosis of choroidal melanomas in the collaborative ocular melanoma study. COMS report no. 1. Arch Ophthalmology 108: 1268-1273.
7. Collaborative Ocular Melanoma Study Group (2003) Comparison of clinical, echographic and histopathological measurements from eyes with medium-sized choroidal melanoma in the collaborative ocular melanoma study: COMS report no. 21. Arch Ophthalmol 121: 1163-1171.
8. Shields CL, Shields JA, Perez N, Singh AD, Cater J (2002) Primary transpupillary thermotherapy for small choroidal melanoma in 256 consecutive cases: Outcomes and limitations. Ophthalmology 109: 225-234.
9. Barbazetto IA, Lee TC, Rollins IS, Chang S, Abramson DH (2003) Treatment of choroidal melanoma using photodynamic therapy. Am J Ophthalmol 135: 898-899.
10. Seddon JM, Gragoudas ES, Polivogianis L, Hsieh CC, Egan KM et al. (1986) Visual outcome after proton beam irradiation of uveal melanoma. Ophthalmology 93: 666-674.
11. Sagoo MS, Shields CL, Mashayekhi A, Freire J, Emrich J, et al. (2011) Plaque radiotherapy for juxtapapillary choroidal melanoma: Tumor control in 650 consecutive cases. Ophthalmology 118: 402-407.
12. Jampol LM, Moy CS, Murray TG, Reynolds SM, Albert DM, et al. (2002) The COMS randomized trial of iodine 125 brachytherapy for choroidal melanoma: IV. Local treatment failure and enucleation in the first 5 years

after brachytherapy. COMS report no. 19. Ophthalmology 109: 2197-2206.

13. Hawkins BS, Collaborative Ocular Melanoma Study Group (2004) The Collaborative Ocular Melanoma Study (COMS) randomized trial of pre-enucleation radiation of large choroidal melanoma: IV. Ten year mortality findings and prognostic factors. COMS report number 24. Am J Ophthalmol 138: 936-951.
14. Emara K, Weisbrod DJ, Sahgal A, McGowan H, Jaywant S, et al. (2004) Stereotactic radiotherapy in the treatment of juxtapapillary choroidal melanoma: Preliminary results. Int J Radiat Oncol Biol Phys 59: 94-100.
15. Krema H, Somani S, Sahgal A, Xu W, Heydarian M, et al. (2009) Stereotactic radiotherapy for treatment of juxtapapillary choroidal melanoma: 3 year follow-up. Br J Ophthalmol 93: 1172-1176.
16. Nag S, Quivey JM, Earle JD, Followill D, Fontanesi J, et al. (2003) The American Brachytherapy Society recommendations for brachytherapy of uveal melanomas. Int J Radiat Oncol Biol Phys 56: 544-555.
17. Müller-Forell W, Wibke S (2003) Imaging of orbital and visual pathway pathology. Springer-Verlag Berlin Heidelberg.
18. Peyster RG, Augsburger JJ, Shields JA, Satchell TV, Markoe AM, et al. (1985) Choroidal melanoma: Comparison of CT, fundoscopy and US. Radiology 156: 675-680.
19. Mafee MF, Peyman GA, McKusick MA (1985) Malignant uveal melanoma and similar lesions studied by computed tomography. Radiology 156: 403-408.
20. Hosten N, Bornfeld N, Wassmuth R, Lemke AJ, Sander B, et al. (1997) Uveal melanoma: Detection of extra ocular growth with MR imaging and US. Radiology 202: 61-67.
21. Mafee MF (1998) Uveal melanoma, choroidal hemangioma and simulating lesions. Role of MR imaging. Radiol Clin North Am 36: 1083-1099.
22. Houle V, Belair M, Allaire GS (2011) AIRP best cases in radiologic-pathologic correlation: Choroidal melanoma. Radiographics 31: 1231-1236.